

# Risk of misinterpretation of low-spin non-yrast bands as wobbling bands

S. Guo,<sup>1,2</sup> X. H. Zhou,<sup>1,2,\*</sup> C. M. Petrache,<sup>3</sup> E. A. Lawrie,<sup>4,5</sup> S. Mthembu,<sup>4,5</sup> Y. D. Fang,<sup>1,2</sup> H. Y. Wu,<sup>6</sup> H. L. Wang,<sup>7</sup> H. Y. Meng,<sup>7</sup> G. S. Li,<sup>1,2</sup> Y. H. Qiang,<sup>1</sup> J. G. Wang,<sup>1,2</sup> M. L. Liu,<sup>1,2</sup> Y. Zheng,<sup>1,2</sup> B. Ding,<sup>1,2</sup> W. Q. Zhang,<sup>1,2</sup> A. Rohilla,<sup>1</sup> K. R. Mukhi,<sup>1</sup> Y. Y. Yang,<sup>1,2</sup> H. J. Ong,<sup>1,2</sup> J. B. Ma,<sup>1,2</sup> S. W. Xu,<sup>1,2</sup> Z. Bai,<sup>1,2</sup> H. L. Fan,<sup>8</sup> J. F. Huang,<sup>9</sup> J. H. Li,<sup>1</sup> J. H. Xu,<sup>1</sup> B.F. Lv,<sup>1</sup> W. Hua,<sup>10</sup> Z. G. Gan,<sup>1,2</sup> and Y. H. Zhang<sup>1,2</sup>

<sup>1</sup>*CAS Key Laboratory of High Precision Nuclear Spectroscopy,  
Institute of Modern Physics, Chinese Academy of Sciences, Lanzhou 730000, China*

<sup>2</sup>*School of Nuclear Science and Technology, University of Chinese  
Academy of Science, Beijing 100049, People's Republic of China*

<sup>3</sup>*Université Paris-Saclay, CNRS/IN2P3, IJCLab, 91405 Orsay, France*

<sup>4</sup>*Themba LABS, National Research Foundation, PO Box 722, 7131 Somerset West, South Africa*

<sup>5</sup>*Department of Physics & Astronomy, University of the Western Cape, P/B X17, Bellville ZA-7535, South Africa*

<sup>6</sup>*State Key Laboratory of Nuclear Physics and Technology,  
School of Physics, Peking University, Beijing 100871, China*

<sup>7</sup>*School of Physics and Microelectronics, Zhengzhou University, Zhengzhou 450001, China*

<sup>8</sup>*College of Engineering Physics, Shenzhen Technology University, Shenzhen 518118, China*

<sup>9</sup>*Guangzhou Municipal Ecological Environment Bureau Huadu District Branch, Guangzhou 510800, People's Republic of China*

<sup>10</sup>*Sino-French Institute of Nuclear Engineering and Technology, Sun Yat-Sen University, Zhuhai 519082, China*

(Dated:)

It is argued that the experimental criteria recently used to assign wobbling nature to low-spin bands in several nuclei are insufficient and risky. New experimental data involving angular distribution and linear polarization measurements on an excited band in <sup>187</sup>Au, previously interpreted as longitudinal wobbling, are presented. The new data show that the linking transitions have dominant magnetic nature and exclude the wobbling interpretation.

PACS numbers: 21.10.Re, 21.60.Ev, 23.20.Lv, 27.60.+j

Although the atomic nucleus is a complicated quantum many-body system its motion often resembles that of a simple physical system in the macroscopic world. Half a century ago it has been predicted, based on the Unified Model, that similar to the precession of a gyroscope in classical mechanics nuclear wobbling exists in deformed triaxial nuclei [1]. When the nucleus wobbles the principle nuclear axis having the largest moment of inertia plays the role of the axle of a gyroscope, and rotates around the space-fixed angular momentum. The wobbling in nuclei is based on the excitation of wobbling phonons, thus it exhibits a quantization of the excitation energies and transition probabilities [1]. Nuclear wobbling was first identified two decades ago, when a series of wobbling bands called triaxial superdeformed (TSD) bands, were observed in several nuclei of the 160 mass region [2–7].

Recently, following the introduction of longitudinal and transverse wobbling by Frauendorf and Döna [8] new cases of wobbling bands have been reported. This new interpretation describes a system based on a rotating triaxial core coupled to an odd quasiparticle, assuming that the moments of inertia of the triaxial core are of hydrodynamic type and the angular momentum of the odd quasiparticle is rigidly aligned with one of the principal axes, (called frozen approximation). Angular momentum coupling of longitudinal (transverse) type is formed where the quasiparticle angular momentum is oriented parallel (perpendicular) to the rotational axis with the

largest moment of inertia. The wobbling equations approximate the unfavoured rotation of a triaxial nucleus as an excitation of wobbling phonons. They furnish an explanation of the observed decreasing trend of the relative excitation energy of the yrare band (wobbling frequency) in some nuclei as resulting from the proposed transverse wobbling, while for simple wobblers or for longitudinal wobbling the wobbling frequency increases. Later a debate about the validity of this picture followed mainly because the effect of the Coriolis force on the odd nucleon in the transverse coupling is neglected in the frozen transverse approximation [9–11]. All recently reported wobbling bands were interpreted using this approximation, for instance several excited bands in <sup>135</sup>Pr, <sup>105</sup>Pd, and <sup>183</sup>Au were interpreted as transverse wobbling [12–15], while the yrare bands in <sup>133</sup>La, <sup>187</sup>Au, and <sup>127</sup>Xe were considered as longitudinal wobbling [16–18].

While the wobbling motion can be considered as a new frontier of low-spin nuclear structure, it is worthwhile to critically assess the evidence supporting such an interpretation. Up to now, all the reported wobbling bands behave like the unfavored signature partners of low- $\Omega$  rotation aligned configurations. In contrast to the interpretation as signature partner bands, the magnitude of the  $E2/M1$  mixing ratios of the  $\Delta I=1$  transitions linking the claimed wobbling bands to the yrast partners is predicted to be larger than 1, therefore predominantly  $E2$ , and is considered as the key experimental criterion. It is worth noting that the large mixing ratios of the con-

necting transitions are only a necessary, but not sufficient condition for wobbling motion, since they cannot be used to exclude some other possible mechanisms, such as the tilted precession [19]. Nevertheless, it would be questionable to regard a sequence of transitions as wobbling band if the alternative nearly zero mixing ratios, leading to predominant  $M1$  character, are not firmly excluded. For all the reported low-spin wobbling bands, the mixing ratios were deduced from angular distribution and/or linear polarization measurements.

Angular distribution curves can be estimated assuming appropriate values for the mixing ratio ( $\delta$ ) and the alignment parameter ( $\sigma/I$ ). It is possible to deduce suitable mixing ratios to get good agreements between estimated curves and experimental results. Usually, two similar curves can be achieved with two mixing ratios  $|\delta_1| > 1$  and  $|\delta_2| < 1$  (see Fig. 1). Therefore, in an angular distribution analysis, one should first find both  $\delta_1$  and  $\delta_2$  solutions by fitting the experimental points, and then plot the two curves together, in comparison with the experimental results. If one curve can meet most experimental points within convincing errors, the corresponding mixing ratio should be regarded as a possible solution. Mixing ratios for the linking transitions of the wobbling bands, extracted from angular distribution measurements have been reported in  $^{135}\text{Pr}$  [12, 13],  $^{133}\text{La}$  [16] and  $^{187}\text{Au}$  [17]. However, in all those works, the curves with  $\delta_2 < 1$  solutions were missing, while those with  $\delta_1 > 1$  values were only compared with pure  $M1$  transitions ( $\delta = 0$ ), leading to a false belief that the correct solution for the mixing ratio is reliably established. Actually, both  $\delta_1$  and  $\delta_2$  can be possible solutions for the two works on  $^{135}\text{Pr}$  and  $^{133}\text{La}$  [12, 16], while they can be both ruled out due to the extremely small errors for the other two on  $^{135}\text{Pr}$  and  $^{187}\text{Au}$  [13, 17] (see Fig. 1). For the latter, it has been not yet demonstrated how to restrict the uncertainty to a negligible level, especially comparing to those of previous works performed using similar experimental setups and statistics [12].

For the angular distribution measurements, sometimes a preferable mixing ratio is suggested based on the  $\chi^2$  fitting. The  $\chi^2$  value is useful to evaluate a fit on directly measurable experimental results. However, the counts for angular distribution analysis are not peak areas measured directly, but deduced from  $\gamma$ - $\gamma$  matrices based on a huge number of independent events. Their central values can be influenced in certain ranges due to the artificial selection of the parameters used in gating and fitting the peak areas. Therefore the  $\chi^2$  value is sensitive to artificial factors, and is less reliable for angular distribution analysis. Furthermore, even if one solution is in disadvantage according to the  $\chi^2$  values, it may not be firmly excluded.

Linear polarization measurements were carried out for  $^{135}\text{Pr}$  [12],  $^{105}\text{Pd}$  [14],  $^{133}\text{La}$  [16],  $^{183}\text{Au}$  [15] and  $^{127}\text{Xe}$  [18]. A series of parameters, such as the asymmetry cor-

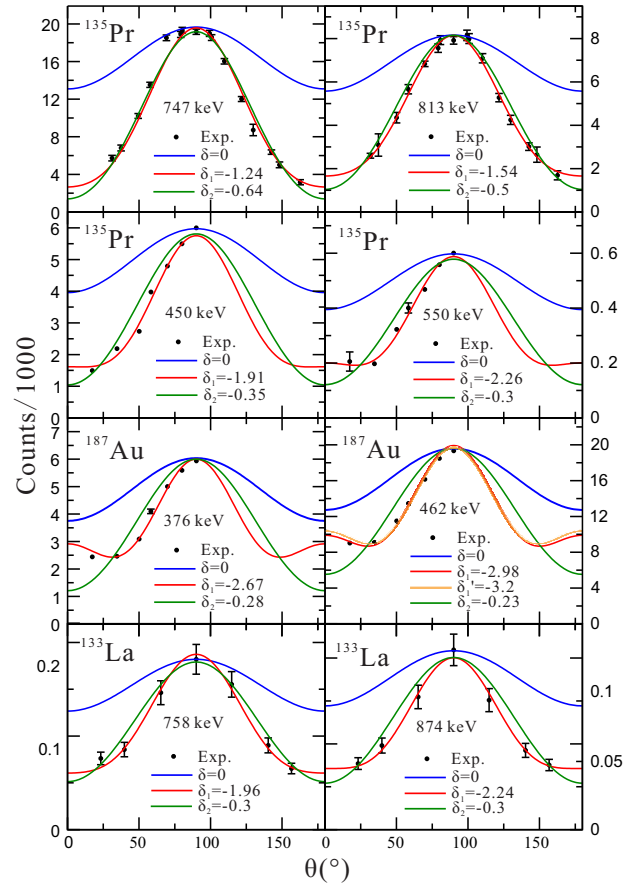


FIG. 1. Estimated angular distribution curves and experimental results for the reported transverse wobbling bands in  $^{135}\text{Pr}$ , and longitudinal wobbling bands in  $^{187}\text{Au}$  and  $^{133}\text{La}$ . The curves for pure  $M1$  transition (in blue) and large  $\delta$  (in red) are taken from the original figures in Refs. [12, 13, 16, 17], and those with smaller mixing ratios and same  $\sigma/I$  are also plotted (in green) for comparison. For the 462-keV transition in  $^{187}\text{Au}$ ,  $\delta = -2.98$  is deduced from the curve marked with  $\delta = -3.2$  in Ref. [17], therefore two curves with the two  $\delta$  values are both plotted.

rection ( $a$ ), the polarization sensitivity ( $Q$ ), and  $\sigma/I$ , should be rigorously calibrated or evaluated to deduce convincing polarization values [20]. However, these essential parameters are not reported for all these works, except the calibration of  $a$  reported in a corresponding PhD thesis on  $^{135}\text{Pr}$  [21]. Furthermore, arguments on gating transition selections and error analysis were also absent from those works. The lack of key experimental information reduces the reliability of the conclusions on the electromagnetic character of the  $\Delta I=1$  linking transitions of the claimed wobbling bands. On the contrary, severe problems have been found in the experimental results on  $^{135}\text{Pr}$  [22] and  $^{133}\text{La}$  [23], which sheds doubts on the assigned wobbling nature to the bands.

Among the reported low-spin wobbling bands, the interpretation for that in  $^{187}\text{Au}$  is most intriguing. To achieve the geometry of the claimed longitudinal wob-

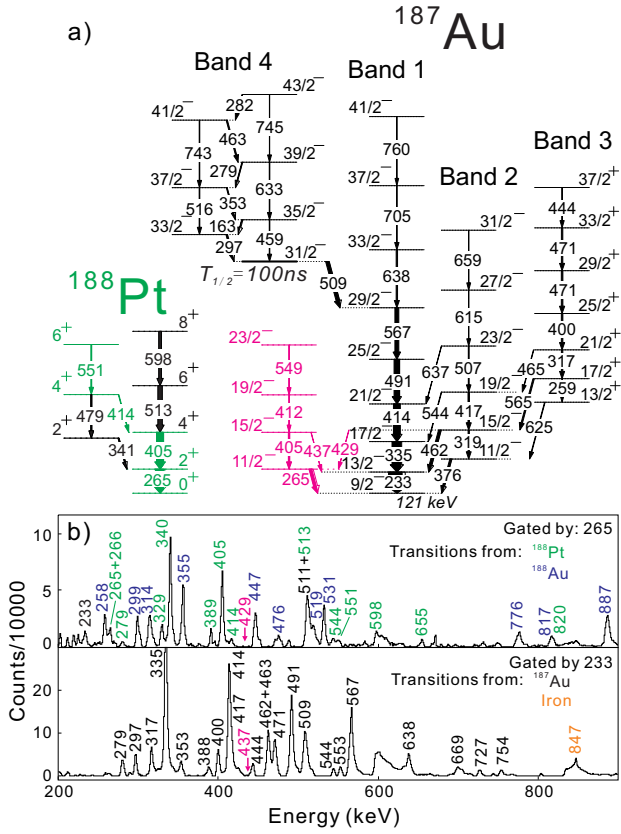


FIG. 2. a) Partial level scheme of  $^{187}\text{Au}$  and  $^{188}\text{Pt}$ . The structure in red was reported in Ref. [17], but not confirmed in the present work. Instead, a sequence in green is found with similar energies which belongs to  $^{188}\text{Pt}$ . b) Typical spectra gated by the 265- and 233-keV transitions.

bling, the quasiproton should be located in the middle of a  $j$ -shell [17], while the proton Fermi surface is close to the bottom of the intruder  $h_{9/2}$  sub-shell [24]. In addition, the large mixing ratios were deduced only from angular distribution measurements, with extremely small errors, while essential experimental information previously published on conversion coefficients from the  $\beta$ -decay of the  $T_{1/2}=2.4$  min,  $J^\pi=13/2^+$  high- $j$  isomer in  $^{187}\text{Hg}$  was ignored [25, 26].

In order to clarify the existing contradictory experimental information and to further investigate the nature of the yrare band in  $^{187}\text{Au}$ , an experiment has been carried out at the Heavy Ion Research Facility in Lanzhou (HIRFL) [27, 28], China. The excited states of  $^{187}\text{Au}$  were studied using the  $^{175}\text{Lu}(^{18}\text{O},6n)$  reaction with a 108-MeV  $^{18}\text{O}$  beam and a stack of two self-supported natural Lu targets with a thickness of 0.7 mg/cm<sup>2</sup> each. The  $\gamma$ -rays were detected by a detector array consisting of 8 segmented clover detectors and 16 coaxial High-purity Germanium (HpGe) detectors. Eight of the HpGe detectors were equipped with anti-Compton shields. All clover detectors were placed in a ring perpendicular to

the beam direction. The 16 HpGe detectors were placed in four rings at 26°, 51°, 129° and 154°. Approximately  $5 \times 10^{10}$  double- or higher-fold events have been recorded by a general-purpose digital data acquisition system [29].

Fig. 2a shows a partial level scheme of  $^{187}\text{Au}$  obtained in the present work, together with a partial level scheme of  $^{188}\text{Pt}$ . The structure in red was reported in Ref. [17], and interpreted as the unfavored signature branch of the  $\pi h_{9/2}$  band (band 1) in  $^{187}\text{Au}$ . However, the sequence including the 265-, 405-, 412, and 549-keV transitions have very similar energies to the 265-, 405-, 414-, 551-keV transitions in the ground state band and the  $\gamma$  band in  $^{188}\text{Pt}$  [30] (the sequence in green in Fig. 2a). Our data shows no sign of the previously proposed linking transitions of 429 keV and 437 keV, (see for instance the spectra gated by the transitions below in Fig. 2b). Therefore, the present work does not support the existence of such a band in  $^{187}\text{Au}$ .

The mixing ratios of the transitions linking band 2 to band 1 reported in the present work are deduced using two complementary measurements of a two-point angular-correlation ratio,  $R_{ac}$ , and of linear polarization,  $P$ .  $R_{ac}$  was deduced from the ratio of the  $\gamma$ -ray intensities measured in the spectra of the 26° and 90° detectors, gated on transitions observed in all detectors. The linear polarization,  $P$ , was deduced based on the Compton scattering events in two adjacent crystals of the clover detectors. The supplementary material provides more details on the experimental methods and the experimental uncertainties [31]. Table I summarizes the measured values of  $R_{ac}$  and  $P$  for the linking transitions between

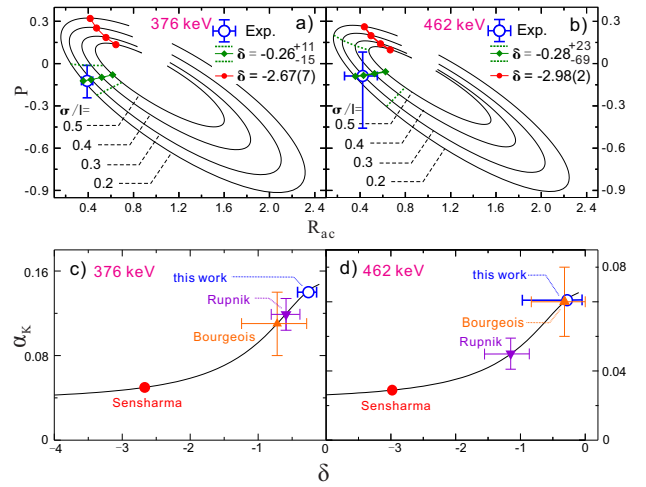


FIG. 3. a & b, Plots for polarization versus  $R_{ac}$  as a function of mixing ratios with different  $\sigma/I$  parameters, together with experimental results and estimated results for certain mixing ratios. c & d, Internal conversion coefficients as a function of mixing ratios, together with the experimental results from the present work and those from Bourgeois, *et al.* [25], Rupnik, *et al.* [26] and Sensharma, *et al.* [17].

TABLE I. Energies of transitions ( $E_\gamma$ ), spin and parities of initial and final states ( $I_i^\pi \rightarrow I_f^\pi$ ), angular correlation ratios ( $R_{ac}$ ), linear polarization coefficients ( $P$ ), E2/M1 mixing ratios ( $\delta$ ) for linking transitions between bands 1 and 2 in  $^{187}\text{Au}$ , and the reduced transition probability ratios between these transitions and inband E2 transitions depopulating the same states.

| $E_\gamma(\text{keV})$ | $I_i^\pi \rightarrow I_f^\pi$ | $R_{ac}$           | $P$                 | $\delta$                       | $B(M1)_{out}/B(E2)_{in}$ | $B(E2)_{out}/B(E2)_{in}$ |
|------------------------|-------------------------------|--------------------|---------------------|--------------------------------|--------------------------|--------------------------|
| 376                    | $11/2^- \rightarrow 9/2^-$    | 0.39(5)            | $-0.12^{+11}_{-12}$ | $-0.26^{+11}_{-16}$            |                          |                          |
| 462                    | $15/2^- \rightarrow 13/2^-$   | $0.42^{+13}_{-16}$ | $-0.09^{+17}_{-37}$ | $-0.28^{+23}_{-69}$            | $0.045^{+9}_{-23}$       | $0.024^{+152}_{-23}$     |
| 544                    | $19/2^- \rightarrow 17/2^-$   |                    |                     | $-0.4^{+4}_{-21}$ <sup>a</sup> | $0.016^{+2}_{-14}$       | $0.012^{+63}_{-12}$      |
| 637                    | $23/2^- \rightarrow 21/2^-$   |                    |                     |                                |                          |                          |

a) Deduced from the reported internal conversion coefficients reported in Ref. [26]

bands 2 and 1. The measured polarization of the 376-keV transition is in good agreement with the value of  $-0.10(5)$  reported earlier [24]. The mixing ratios were deduced from the measured values of  $R_{ac}$  and  $P$  using the ellipse-like curves calculated as a function of  $\delta$ , shown in Fig. 3. The curves are sensitive to the  $\sigma/I$  parameter, which is usually assumed to be 0.3. However its value can be affected by states with lifetimes of the order of a picosecond or larger which are usually present in the low-spin region. Furthermore, in  $^{187}\text{Au}$  there is a 100-ns isomer, which partially decays towards the states of band 1 (see Fig. 2). Due to the induced uncertainties by the  $\sigma/I$  parameter we estimate the experimental error bars of the mixing ratios assuming that  $\sigma/I$  may cover the range of 0 - 1. Despite the large error bars it is clear that the absolute values of the deduced mixing ratios are smaller than 1 confirming the dominant  $M1$  nature of these transitions. Data points that correspond to the large mixing ratios deduced in Ref. [17] are shown in red in Fig. 3. They are in distinct disagreement with both the presently deduced values and with the values obtained from previous internal conversion coefficients measurements [25, 26] (see Fig. 3).

The experimentally measured reduced transition probability ratios of  $B(E2)_{out}/B(E2)_{in}$  extracted from the present data are listed in Table I. Taking into account the low values of these ratios and that  $B(E2)_{in}$  values in the collective bands of  $^{187}\text{Au}$  are expected to be  $\approx 100$  - 200 W.u. (as the  $B(E2)$  for the  $2^+ \rightarrow 0^+$  transition in  $^{186}\text{Pt}$  is  $94 \pm 5$  W.u. [32], while the  $B(E2)$  for the 233-keV  $13/2^- \rightarrow 9/2^-$  transition in  $^{187}\text{Au}$  is  $188 \pm 17$  W.u. [33]), the expected values of  $B(E2)_{out}$  are only a few W.u., which is inconsistent with wobbling and in general does not support collective type of excitation. In order to study further the nature of band 2, one-quasiparticle-plus-triaxial-rotor (QTR) model calculations were carried out.

The present QTR model calculations use the codes of P. Semmes and I. Ragnarsson [34]. Standard parameters are used for the Nilsson potential [35] and for the pairing strength. The moments of inertia of the core have irrotational-flow nature, as suggested by an empirical evaluation [36]. The spin dependence is taken into account by assuming variable moments of inertia described

by the Harris parameters  $J_0 = 25 \hbar^2 \text{MeV}^{-1}$  and  $J_1 = 8 \hbar^4 \text{MeV}^{-3}$ . The adopted quadrupole deformation of  $\varepsilon = 0.21$  is similar to that previously used in Refs. [17, 26]. The adopted triaxial deformation is  $\gamma = 12^\circ$ , as found in the theoretical calculations for  $^{186}\text{Pt}$  [37] (for more details see the supplementary material [31]). The calculated proton Fermi level is near the highest  $h_{11/2}$  and lowest  $h_{9/2}$  orbitals, as in Ref. [24]. The 9 negative-parity orbitals closest to the Fermi level are included in the calculations. They involve orbitals with  $h_{9/2}$ ,  $f_{7/2}$  and  $h_{11/2}$  origin.

The calculated excitation energies of the two lowest-energy rotational bands with  $h_{9/2}$  nature are shown in Fig. 4. The yrast band is based on dominant single-particle contribution from the lowest-energy  $h_{9/2}$  orbital. The yrare band corresponds to dominant contribution from the second lowest-energy  $h_{9/2}$  orbital, suggesting that the yrare band corresponds to a non-collective excitation. More details on the specifics of the wave functions are given in the supplementary material.

The calculated mixing ratios are in good agreement

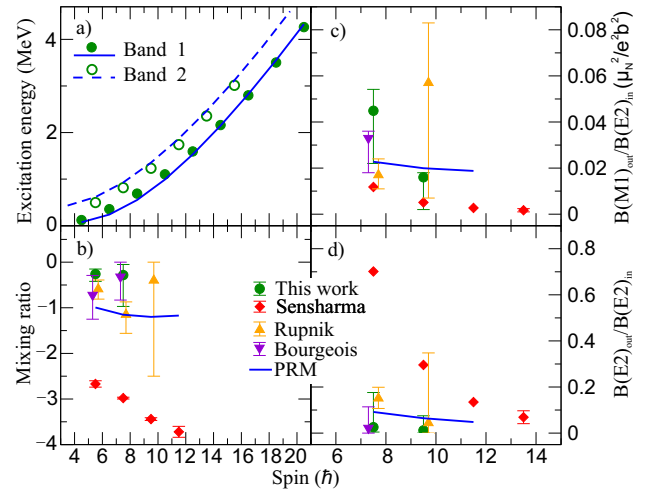


FIG. 4. Experimental and theoretical results for the excitation energies (a), mixing ratios (b),  $B(M1)_{out}/B(E2)_{in}$  ratios (c) and  $B(E2)_{out}/B(E2)_{in}$  ratios (d) for bands 1 and 2 of  $^{187}\text{Au}$ . The values of previously measured mixing ratios [17, 24–26], are also shown.



with our data and with data from Refs. [24–26], but in contrast with the data from Ref. [17] (see Fig. 4b). The calculations also predict relatively low values for the  $B(E2)_{out}/B(E2)_{in}$  ratios for the yrare band, and are in good agreement with the data of the present experiment, further supporting the proposed non-collective character of the band.

In summary, the recently reported longitudinal wobbling band in  $^{187}\text{Au}$  is re-investigated via an experiment involving angular distribution and linear polarization measurements. The deduced low mixing ratios for the linking transitions between the yrare and the yrast bands are in disagreement with the high values reported by Sensharma et al. [17], but in agreement with the conversion coefficients reported by Bourgeois et al. [25] and Rupnik et al. [26], and with linear polarization value reported by Bourgeois et al. [24]. These mixing ratios indicate low  $B(E2)_{out}/B(E2)_{in}$  ratios and show that the yrare band is not produced by a collective excitation, ruling out the longitudinal wobbling interpretation proposed in Ref. [17]. Quasiparticle-plus-triaxial-rotor-model calculations reproduce well the experimental data. The calculations show that the yrast (yrare) band are associated with the lowest- (second-lowest)  $h_{9/2}$  orbital, indicating that the yrare band is generated predominantly by a single-particle excitation.

The deduced small values of the mixing ratios in  $^{187}\text{Au}$  in contrast with the previously published data in Ref. [17] underline the risk of misinterpretation of yrare band as wobbling if one incorrectly select the  $|\delta| > 1$  mixing ratio. This risk, also highlighted by the concerns about the mixing ratio measurements in  $^{135}\text{Pr}$  [22] and  $^{133}\text{La}$  [23], put forward the need to re-measure the mixing ratios for other candidate wobbling bands too. Furthermore, the large mixing ratios are indicative of collective excitation, but not necessarily of wobbling motion, which requires the observation of quantization in the excitation energies and reduced transition probabilities, as a basic feature of all phonon excitations. One can conclude that more experimental and theoretical works are needed to clarify the nature of the low-spin yrare bands, which otherwise risk to be misinterpreted as wobbling bands.

The authors would like to thank the accelerator crew of HIRFL for providing the stable  $^{18}\text{O}$  beam during the pandemic of COVID-19. This work has been supported by the National Key R&D Program of China (Contract Nos. 2018YFA0404402, 2018YFA0404400 and 2017YFE0116700), the Key Research Program of the Chinese Academy of Sciences (Grant No. XDPB09-02), the National Natural Science Foundation of China (Grant Nos. U1932137, U1732139, U1832134, 11775274, 11975209, and 11805289), the Cai Yuanpei 2018 Project No. 41458XH, and the National Research Foundation of South Africa, GUN: 93531, 109134.

---

\* Corresponding author; [zxh@impcas.ac.cn](mailto:zxh@impcas.ac.cn)

- [1] A. Bohr and B. R. Mottelson, **Nuclear Structure (Benjamin, New York, 1975), Vol. II.** (1975).
- [2] S. W. Ødegård, G. B. Hagemann, D. R. Jensen, M. Bergström, B. Herskind, and G. Sletten *et al.*, *Phys. Rev. Lett.* **86**, 5866 (2001).
- [3] D. R. Jensen, G. B. Hagemann, I. Hamamoto, S. W. Ødegård, B. Herskind, and G. Sletten *et al.*, *Phys. Rev. Lett.* **89**, 142503 (2002).
- [4] P. Bringel, G. B. Hagemann, H. Hübel, A. Al-khatib, P. Bednarczyk, and A. Bürger *et al.*, *The European Physical Journal A - Hadrons and Nuclei* **24**, 167 (2005).
- [5] G. Schönwaßer, H. Hübel, G. Hagemann, P. Bednarczyk, G. Benzoni, and A. Bracco *et al.*, *Physics Letters B* **552**, 9 (2003).
- [6] H. Amro, W. Ma, G. Hagemann, R. Diamond, J. Domscheit, and P. Fallon *et al.*, *Physics Letters B* **553**, 197 (2003).
- [7] D. J. Hartley, R. V. F. Janssens, L. L. Riedinger, M. A. Riley, A. Aguilar, and M. P. Carpenter *et al.*, *Phys. Rev. C* **80**, 041304 (2009).
- [8] S. Frauendorf and F. Dönau, *Phys. Rev. C* **89**, 014322 (2014).
- [9] K. Tanabe and K. Sugawara-Tanabe, *Phys. Rev. C* **95**, 064315 (2017).
- [10] S. Frauendorf, *Phys. Rev. C* **97**, 069801 (2018).
- [11] K. Tanabe and K. Sugawara-Tanabe, *Phys. Rev. C* **97**, 069802 (2018).
- [12] J. T. Matta, U. Garg, W. Li, S. Frauendorf, A. D. Ayangeakaa, and D. Patel *et al.*, *Phys. Rev. Lett.* **114**, 082501 (2015).
- [13] N. Sensharma, U. Garg, S. Zhu, A. Ayangeakaa, S. Frauendorf, and W. Li *et al.*, *Physics Letters B* **792**, 170 (2019).
- [14] J. Timár, Q. B. Chen, B. Kruzsicz, D. Sohler, I. Kuti, and S. Q. Zhang *et al.*, *Phys. Rev. Lett.* **122**, 062501 (2019).
- [15] S. Nandi, G. Mukherjee, Q. B. Chen, S. Frauendorf, R. Banik, and S. Bhattacharya *et al.*, *Phys. Rev. Lett.* **125**, 132501 (2020).
- [16] S. Biswas, R. Palit, S. Frauendorf, U. Garg, W. Li, and G. H. Bhat *et al.*, *The European Physical Journal A* **55**, 159 (2019).
- [17] N. Sensharma, U. Garg, Q. B. Chen, S. Frauendorf, D. P. Burdette, and J. L. Cozzi *et al.*, *Phys. Rev. Lett.* **124**, 052501 (2020).
- [18] S. Chakraborty, H. Sharma, S. Tiwary, C. Majumder, A. Gupta, and P. Banerjee *et al.*, *Physics Letters B* **811**, 135854 (2020).
- [19] E. A. Lawrie, O. Shirinda, and C. M. Petrache, *Phys. Rev. C* **101**, 034306 (2020).
- [20] K. Starosta, T. Morek, C. Droste, S. Rohoziński, J. Srebrny, and A. Wierzychucka *et al.*, *Nucl. Instrum. Methods Phys. Res., Sect. A* **423**, 16 (1999).
- [21] J. T. Matta, *Springer Theses ph.D thesis*.
- [22] S. Guo, C. Petrache, and E. Lawrie, *arXiv* **2007** (2020).
- [23] W. Hua, S. Guo, C. Petrache, and E. Lawrie, *arXiv* **2007** (2020).
- [24] C. Bourgeois, M. G. Porquet, N. Perrin, H. Sergolle, F. Hannachi, G. Bastin, and F. Beck, *Zeitschrift für Physik A Atomic Nuclei* **333**, 5 (1989).

- [25] C. Bourgeois, P. Kilcher, J. Letessier, V. Berg, and M. Desthuilliers, [Nuclear Physics A \*\*295\*\*, 424 \(1978\)](#).
- [26] D. Rupnik, E. F. Zganjar, J. L. Wood, P. B. Semmes, and P. F. Mantica, [Phys. Rev. C \*\*58\*\*, 771 \(1998\)](#).
- [27] J. Xia, W. Zhan, B. Wei, Y. Yuan, M. Song, and W. Zhang *et al.*, [Nucl. Instrum. Methods Phys. Res., Sect. A \*\*488\*\*, 11 \(2002\)](#).
- [28] Z. Sun, W.-L. Zhan, Z.-Y. Guo, G. Xiao, and J.-X. Li, [Nucl. Instrum. Methods Phys. Res., Sect. A \*\*503\*\*, 496 \(2003\)](#).
- [29] H. Wu, Z. Li, H. Tan, H. Hua, J. Li, and W. Hennig *et al.*, [Nucl. Instrum. Methods Phys. Res., Sect. A \*\*975\*\*, 164200 \(2020\)](#).
- [30] S. Mukhopadhyay, D. C. Biswas, S. K. Tandel, S. Frauenthorf, L. S. Danu, and P. N. Prashanth *et al.*, [Phys. Rev. C \*\*96\*\*, 014315 \(2017\)](#).
- [31] See Supplementary Material for more details.
- [32] C. M. BAGLIN, [Nuclear Data Sheets \*\*99\*\*, 1 \(2003\)](#).
- [33] M. Basunia, [Nuclear Data Sheets \*\*110\*\*, 999 \(2009\)](#).
- [34] P. B. Semmes and I. Ragnarsson, in *Proceedings of the International Conference on High-Spin Physics and Gamma-Soft Nuclei, Pittsburg, 1990*, edited by J. X. Saladin, R. A. Sorenson, and C.M.Vincent (World Scientific, Singapore, 1991), p. 500; in *Future Directions in Nuclear Physics with  $4\pi$  Gamma Detection Systems of the New Generation*, edited by J. Dudek and B. Haas (AIP Conf. Proc. 259, 1992), p. 566.
- [35] T. Bengtsson and I. Ragnarsson, [Nuclear Physics A \*\*436\*\*, 14 \(1985\)](#).
- [36] J. Allmond and J. Wood, [Physics Letters B \*\*767\*\*, 226 \(2017\)](#).
- [37] R. Rodríguez-Guzmán, P. Sarriguren, L. M. Robledo, and J. E. García-Ramos, [Phys. Rev. C \*\*81\*\*, 024310 \(2010\)](#).